Strength of Tubular Hollow Steel Sections Beams Externally Reinforced by Carbon FRP Sheets

Muna H. Jaber
Babylon University/ Civil Eng.

Abstract

The experimental research reported is aimed using small quantities of CFRP strips to provide tubular section against local buckling for (five) specimens of steel beams.The tubular hollow steel beams sections are made from welding thin plates at their edges. The use of high-strength advanced composite materials tends to accompany the minimum of structural weight, and is hence presently being assessed for effectiveness as supplementary external reinforcing materials. Composite beams of fiber-reinforced polymers (FRP) and steel formed as tubular steel sections externally reinforced by thin-bonded carbon FRP (CFRP) sheets, exhibit many phenomena not found in conventional structural steel components, and these can have a marked bearing both on the behavior of members composed of these materials and, by connotation, on the way in which such members are designed. The type of strengthen carbon fiber is a unidirectional woven fiber mat of mid strength which is a product of Sika coded as SikaWrap-230C. The CFRP is fixed using a resin Sikadure-330.The study is focusing on the local stability of such members. Also formulation of the finite element method used for analyzing the tested beams. The finite element model will be using the experimental load-deflection results of the steel beams. The use of ANSYS-9 to create the finite element model is adopted, the maximum different between experimental results and ANSYS-9 results is 8.7%.

الخلاصة

تم تحري السلوك ألمختبري باستعمال كمية قليلة من شرائح ألياف الكربون البوليمري (CFRP) لتحسين أداء الانحناء الموضعي للعتبات الحديدية المجوفة. تم تصنيع نماذج العتبات المجوفة من لحم صفائح نحيفة الجدران نوع التقوية تمت باستعمال حصيرة ألياف كربون منسوجة باتجاه واحد من النوع المتوسط المقاومة إنتاج شركة سيكا ذو الرمز(Sika Wrap-230C). تم تثبيت ألياف الكربون باستعمال راتنج نوع(Sikadure-330). ركزت الدراسة على الاستقرارية الموقعية لمثل هذه الأعضاء. تم اقتراح أنماط عديدة للتقوية.تم استخلاص توصيات لأفضل نمط من ناحية الكفاءة و الاقتصاد. هذه التقنية وفرت إمكانية تذليل الصعوبات المرتبطة بإيجاد تقنية توفر الكلفة والفعالية بأقل ما ممكن من عرقلة للمستخدمين المنشأ.وبطريقة العناصر المحددة تم تحليل العتبات المفحوصة مختبريا. وهذه الطريقة اعتمد على النتائج العملية لمنحني الحمل والهطول للعتبات الحديدية. بالاعتماد على ANSYS-9 تم تطبيق طريقة العناصر المحددة وأقصى فرق بين النتائج العملية ونتائج ANSYS-9 كانت 8.7%.

Introduction

Recent research on the strengthening of circular hollow sections (CHS) with FRP by (Teng and Hu 2007) and (Hong et al. 2000) in axial compression, (Haedir *et al*. 2007,2006) in bending,(Doi *et al*. 2003)in bending and compression, (Jiao and zhao 2004) in tension, and(Zhao *et al* 2005) and (Xiao *et al*. 2005) on concrete filled CHS, have shown significant benefits in strength and stiffness of steel members with externally bonded CFRP. Experiments on steel RHS strengthened with CFRP under transverse end bearing force were described by (Zhao *et al*. 2006). The mechanical properties of reinforced fiber rely on the fiber characteristics, such as their size, the percentage of fiber reinforcement, and the orientations of fibers. One of the greatest limitations to the behavior of conventional steel tubular beams composed of thin section is the susceptibility of the steel component to local buckling. This local instability is more likely to occur in thin than in thick section, and the effect of local stresses within the steel can result in a reduction of strength.

Experimental setup and test specimens

The section dimensions of the specimens produced by seam-welded along length of two parts of steel with 2mm thickness, 180mm diameters of Section of specimen and 765mm length of the beam of 320Mpa yield steel. The measured uni-axial tensile material properties are listed in Table 1. Fig1 shown section of the specimen, Fig2 Shown the distribution Pattern of CFRP of the tested specimens which used in the test.

Table 1: The dimension and the measured uni-axial tension material properties of the Steel sheets which used to fabricate the tubular steel columns.

Specimen	**Thickness *t (mm)***	**Diameter of section (mm)D_1**	**Length l (mm)**	**Yield Stress f_y (Mpa)**	**Ultimate Stress f_u (Mpa)**	**Failure Strain ε_f**
1 to 5	2	180	765	320	400	0.10714

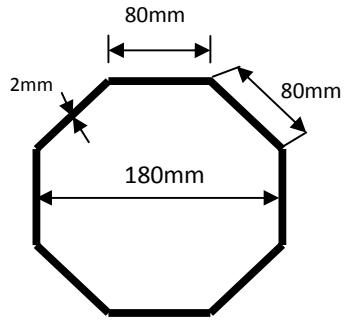

Fig 1: Section of specimen

The tubular steel beams strengthen with different of woven carbon fiber type Sika Wrap-230C by epoxy Sikadure-330 the material properties are tabulated in Table 2.

Table(2) : The material properties of Sika Wrap-230c carbon fiber and Sikadure-330 epoxy.

Material	Fabric design Thickness (mm)	Fiber density g/cm^3	Areal weight g/m	Tensile strength (Mpa)	E-Modulus (Mpa)
Sika Wrao-230C	0.131	1.76	230	4300	238000
Sikadure-330	----	----	----	30	4500

The test program include tested five hollow steel sections, non-strengthen tubular steel beam(TSB). The second tubular steel beam was strengthen by two strips were applied at flat sides on both the tension and compression. The two strips had a width of 50mm and length 70mm (TSB1).The third tubular steel beam was strengthen by six strips.The two strips locate on the center flats had a width 50mm and length 70mm, while the four adjacent strips had a width 50mm and length 60mm(TSB2).The fourth tubular steel beam was strengthen by eight strips. The four strips locate on the center flats had a width 50mm and length 70mm, while the four adjacent strips had a width 50mm and length 60mm (TSB3).The fifth tubular steel beam was strengthen by twelve strips. The four strips locate on the center flats had a width 50mm and length 70mm, while the eight adjacent strips had a width 50mm and length 60mm (TSB4).

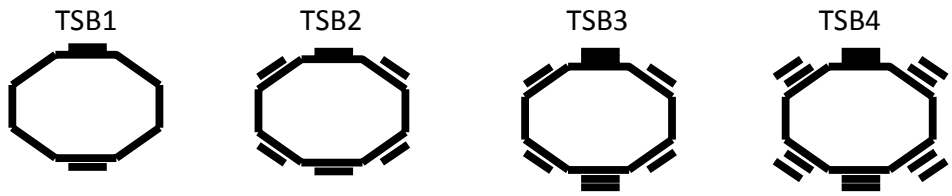

Fig. 2: The distribution Pattern of CFRP of the tested specimens

Finite element modeling

General

The finite element method has become a powerful tool for the numerical solution of a wide range of engineering problems. In this search the formulation of the finite element method used for analyzing the tested columns is introduced. The use of ANSYS-9 to create the finite element model is adopted. All the necessary steps to create the calibrated model are explained in details and the steps taken to generate the analytical load-deflection response of the member are discussed.

Nonlinear finite element analysis for tested beams

Most phenomena in solid mechanics are nonlinear. However in many applications it is convenient and practical to use linear formulation for problems to obtain engineering solutions. On the other hand, some problems definitely require nonlinear analysis if realistic results are to be obtained such as post-yielding and large deflection behavior of structures. Depending on the sources of nonlinearities, the nonlinear problems can be divided into three categories. In brief, these categories are, Problems involving material nonlinearity, Problems involving geometric nonlinearity and Problems involving both materials and geometric nonlinearity.

The present study deals with material nonlinearity in analyzing the tested beams. This is because large deflection behavior of structures. Buckling loads are critical loads where certain types of structures become unstable. Each load has an associated buckled mode shape; this is the shape that the structure assumes in a buckled condition. There are two primary means to perform a buckling analysis:

1-Eigenvalue

Eigenvalue buckling analysis predicts the theoretical buckling strength of an ideal elastic structure. It computes the structural eigenvalues for the given system loading and constraints. This is known as classical Euler buckling analysis. Buckling loads for several configurations are readily available from tabulated solutions. However, in real-life, structural imperfections and nonlinearities prevent most real-world structures from reaching their eigenvalue predicted buckling strength; i.e. it over-predicts the expected buckling loads. This method is not recommended for accurate, real-world buckling prediction analysis.

2-Nonlinear

Nonlinear buckling analysis is more accurate than eigenvalue analysis because it employs non-linear, large-deflection, static analysis to predict buckling loads. Its mode of operation is very simple: it gradually increases the applied load until a load level is found whereby the structure becomes unstable (i.e. suddenly a very small increase in the load will cause very large deflections). The true non-linear nature of this analysis thus permits the modeling of geometric imperfections, load perturbations, material nonlinearities and gaps. For this type of analysis, note that small off-axis loads are necessary to initiate the desired buckling mode.

Finite element representation of steel beams strengthening by external CFRP

In the field of solid mechanics, the finite element method is usually used to find approximate solutions for structures having complicated shapes and /or loading arrangement. The element types for this model are shown in Table (3) . The SOLID45 element was used to model the steel. This element has eight nodes with three degrees of freedom at each node translation in the nodal x, y and z directions the element has plasticity, creep, swelling, stress stiffening, large deflection, and large strain capabilities. A reduced integration option with hourglass control is available.

While Shell41 represents the CFRP strips, SHELL41 is a 3-D element having membrane (in-plane) stiffness but no bending (out-of-plane) stiffness. It is intended for shell structures where bending of the elements is of secondary importance. The element has three degrees of freedom at each node: translations in the nodal x, y, and z directions. The element is defined by four nodes, four thicknesses, a material direction angle and the orthotropic material properties. Orthotropic material directions correspond to the element coordinate directions. The element coordinate system orientation is as described in Coordinate Systems. The element x-axis may be rotated by an angle THETA (in degrees).The element may have variable thickness. The thickness is assumed to vary smoothly over the area of the element, with the thickness input at the four nodes. If the element has a constant thickness, only TK(I) need be input. If the thickness is not constant, all four thicknesses must be input. Parameter needed to define the material models can be founded in Tables(4).

Materials Properties

EX is the modulus of elasticity of the concrete and PRXY is the Poisson's ratio. The bilinear model requires the yield stress as well as the hardening modulus of the steel to be defined.

Table 3: Element types for working model

Material type	ANSYS element
Steel CFRP strips	SOLID45 SHELL41

Table 4: Material models for the calibration model

Material model number	Element Type	Material properties		Real Constant	
1	SOLID45	Linear Isotropic			
		EX	200000		
		PRXY	0.3		
		Bilinear Isotropic			
		Yield stss	280		
		Tang mod	2000		
2	SHEEL41	Linear orthotropic		Shell thickness of node J TK(J)	0.131
		EX	230000		
		EY	1	node K TK(K)	0.131
		EZ	1	node L TK(L)	0.131
		PRXY	0	Element x-axis rotation theta	0°,45°
		PRYZ	0		
		PRXZ	0	Elastic foundation stiffness	0
		GXY	1		
		GYZ	1	Add mass/unite area	0
		GXZ	1		

Experimental and ANSYS results

The test beams were simply supported and loaded under two-point. Load was applied by using an universal testing machine as shown in Fig. (3) . The results show that the application of CFRP to the steel beams increase the stiffness, the ultimate load and decrease the local buckling. The obtained results from experimental tested and ANSYS-9 rate of load application tabulated in Table (5). The applied are load varsus maximum displacement curve for the experimental tested beams are shown in Fig.(9).The curves for each beam experimentaly tested and solved by ANSYS-9 are shown in Fig.(4) to Fig.(8). Beside that, these figures show the shape of beams tested.

Fig. 3: The universal testing machine

Table 5: The experimental and ANSYS-9 results of the tested beam.

Specimen	P_u (KN)	$\frac{Pu - Po}{Po} * 100$	P_A (KN)	$\frac{PA - Pu}{Pu} * 100$
TSB	**23**	**0%**	**24**	**4.35%**
TSB 1	**36**	**56.5%**	**38**	**5.6%**
TSB 2	**43**	**87%**	**44**	**2.32%**
TSB 3	**45**	**95%**	**48**	**2.13%**
TSB 4	**46**	**100%**	**50**	**8.7%**

Where:

P_u : ultimate axial load (KN) by experimental tested.

P_o : ultimate axial load of non-strength steel beam (KN) by experimental tested.

P_A : ultimate axial load (KN) by ANSYS-9 .

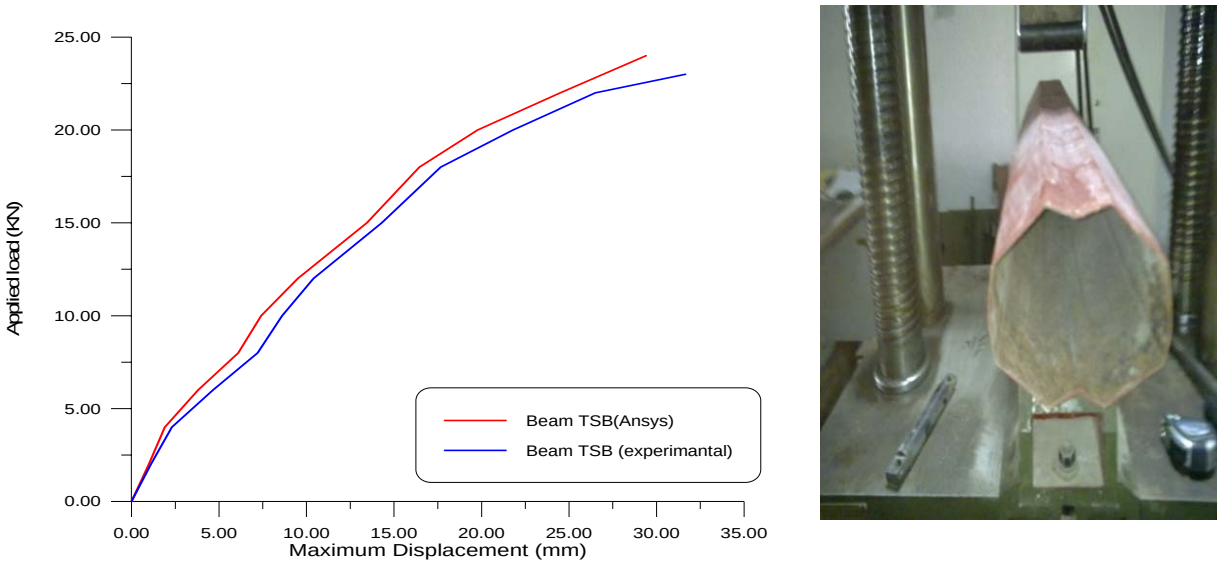

Fig. 4 : The applied load vs to maximum displacement curve of beam TSB by experimental tested and ANSYS -9.

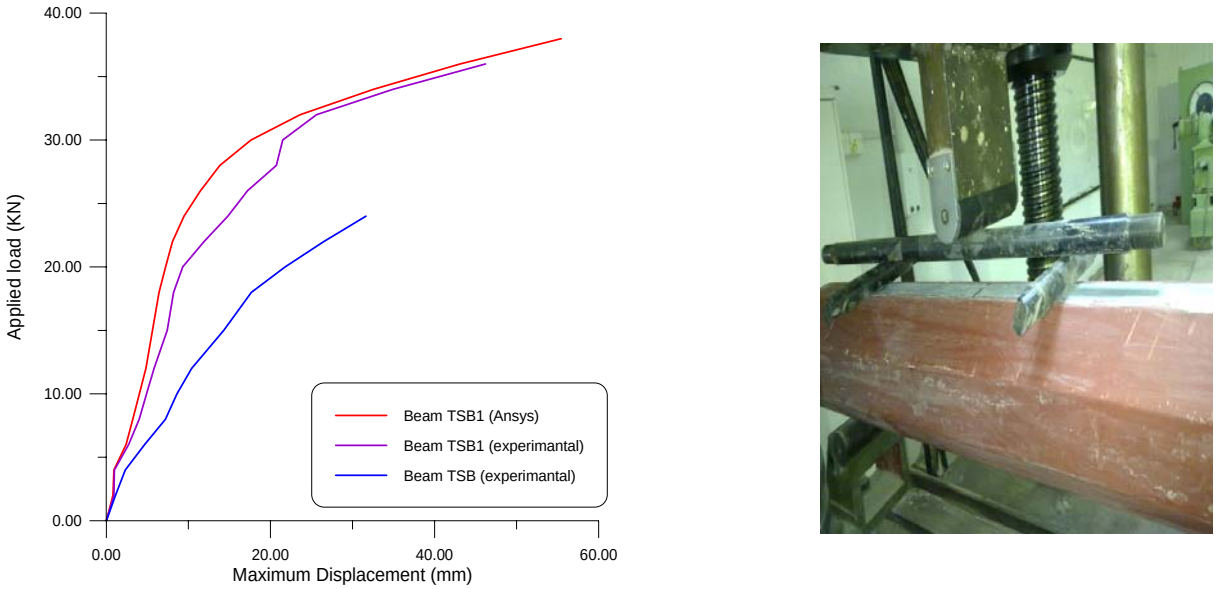

Fig. 5 : The applied load vs to maximum displacement curve of beam TSB1 by experimental tested and ANSYS -9.

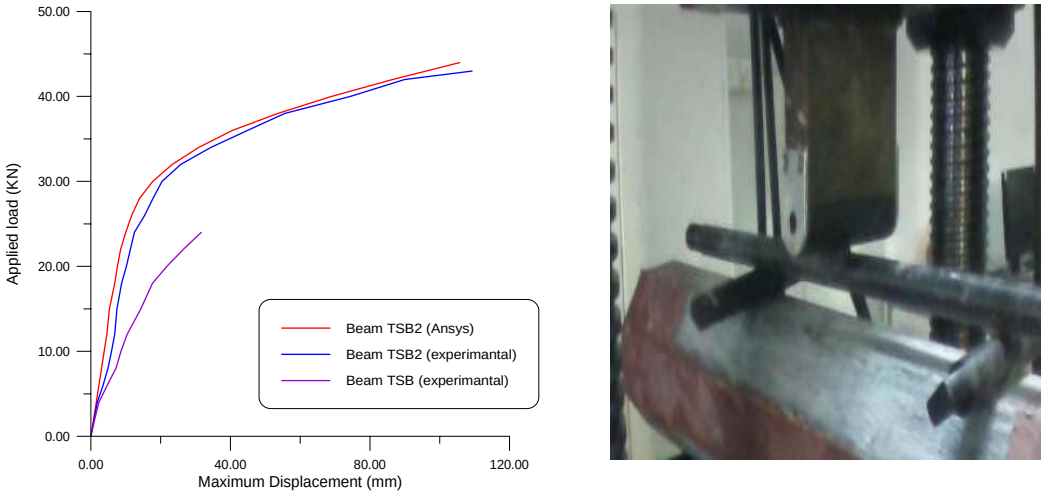

Fig. 6: The applied load vs to maximum displacement curve of beam TSB2 by experimental tested and ANSYS -9

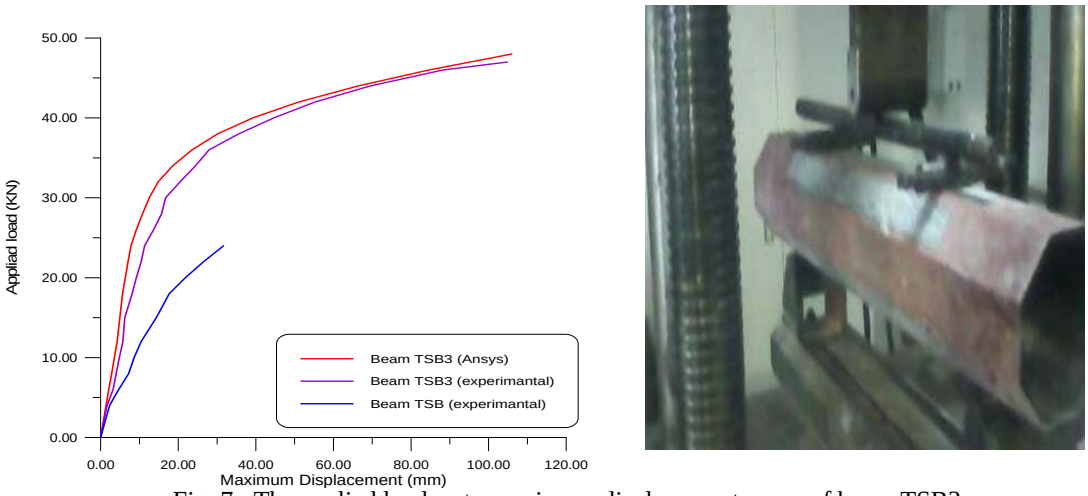

Fig. 7 : The applied load vs to maximum displacement curve of beam TSB3 by experimental tested and ANSYS -9.

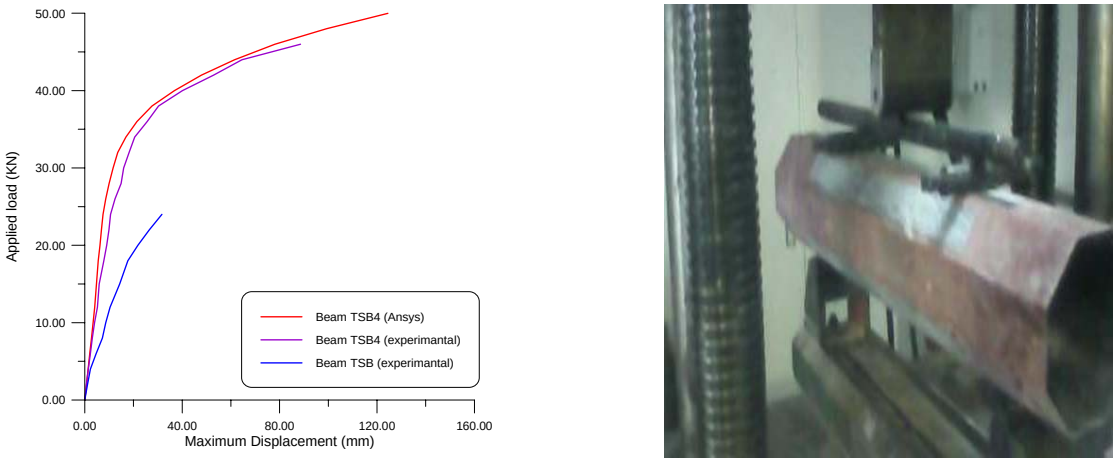

Fig. 8 : The applied load vs to maximum displacement curve of beam TSB4 by experimental tested and ANSYS -9.

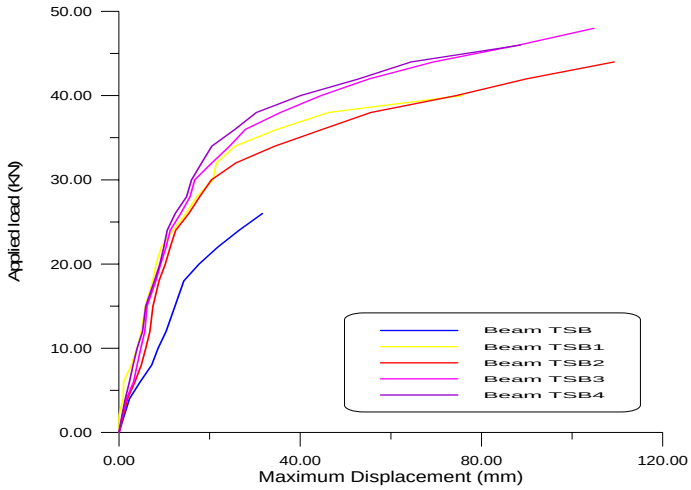

Fig. 9 : The experimental applied load vs to maximum displacement curve of the tested beams.

Fig.(11) shows that the column TSB4 represented the best distribution of CFRP which increased the ultimate load to about (100%). The Figures from (12) to (16) show distribution of stresses intensity, maximum displacement in Y direction and distribution of stresses intensity at CFRP of each beams by ANSYS-9 and bulking of TSB beam shown at Fig.(12).

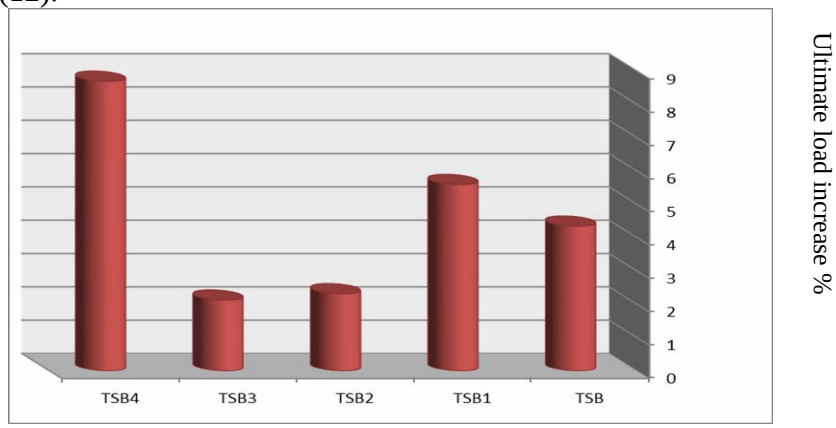

Fig. 10 : % ultimate load increase for beams tested.

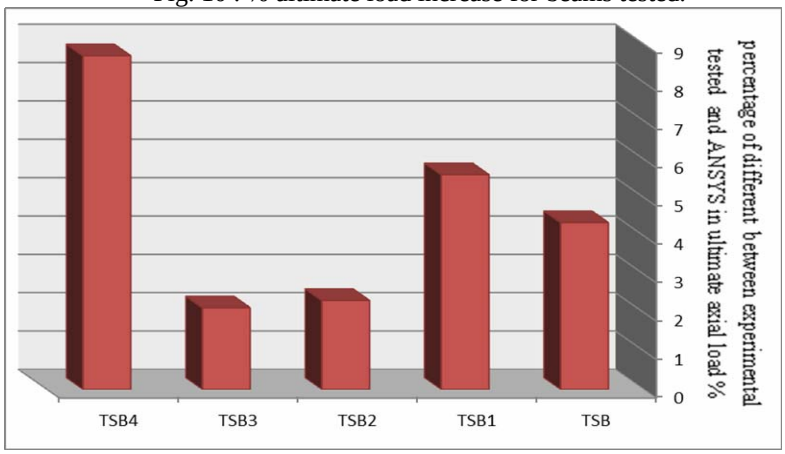

Fig.11 : The percentage of difference between ultimate axial load of experimental tested and ANSYS-9 for beams.

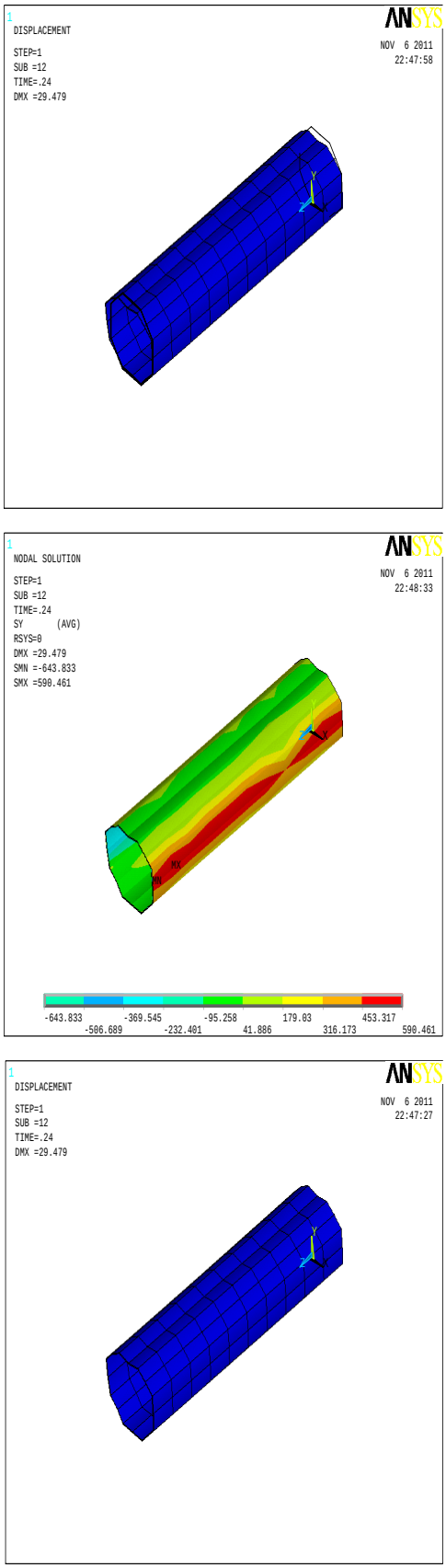

Fig. 12: Distribution of stresses intensity, Maximum displacement in Y direction and bulking of TSB beam by ANSYS-9.

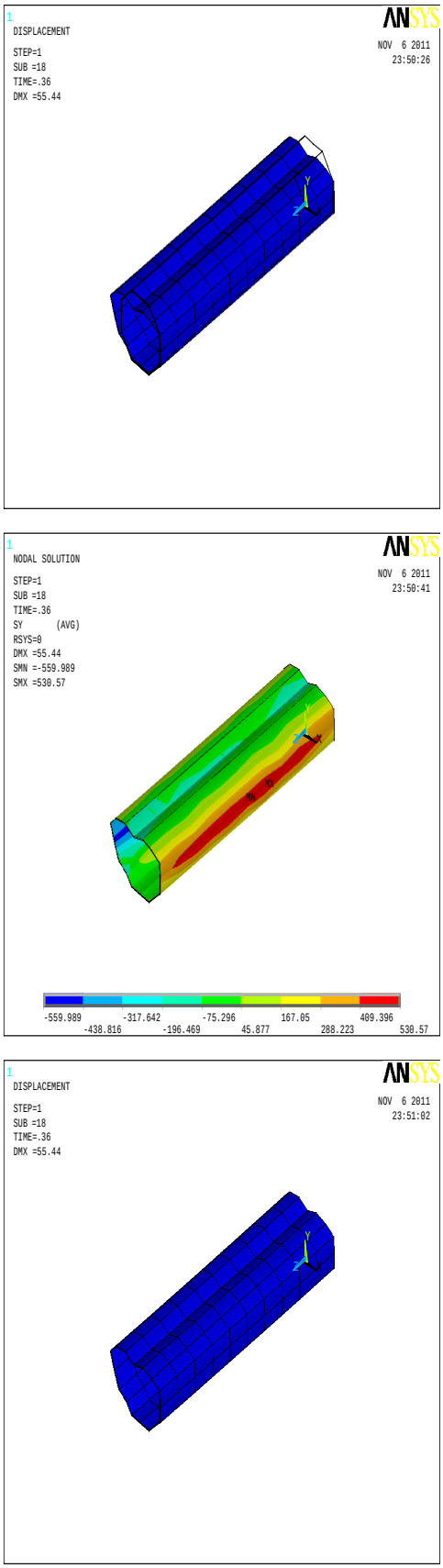

Fig. 13: Distribution of stresses intensity, Maximum displacement in Y direction and bulking of TSB1 beam by ANSYS-9.

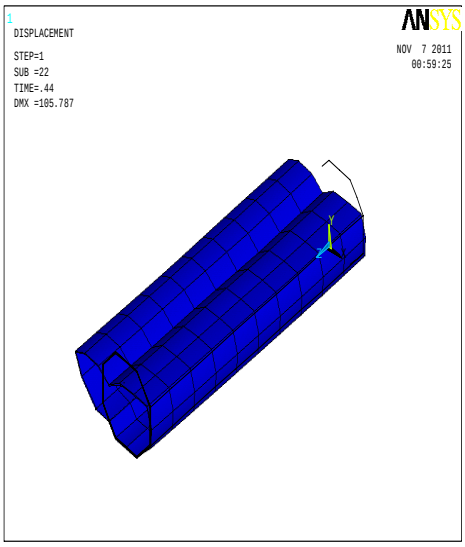

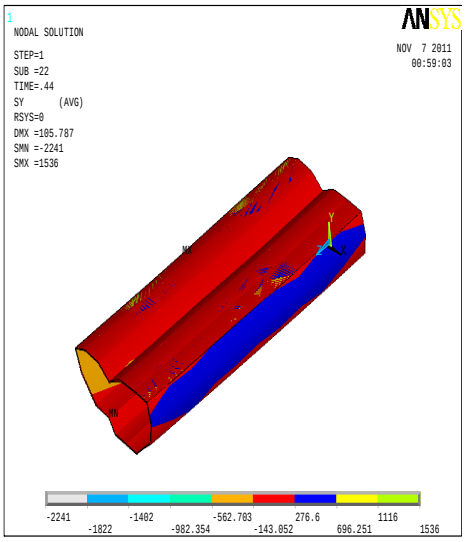

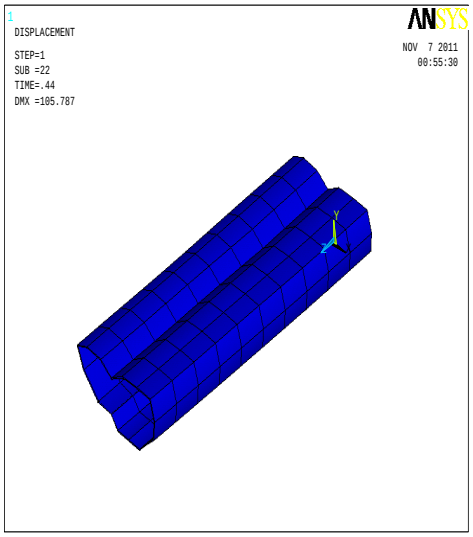

Fig. 14: Distribution of stresses intensity, Maximum displacement in Y direction and bulking of TSB2 beam by ANSYS-9.

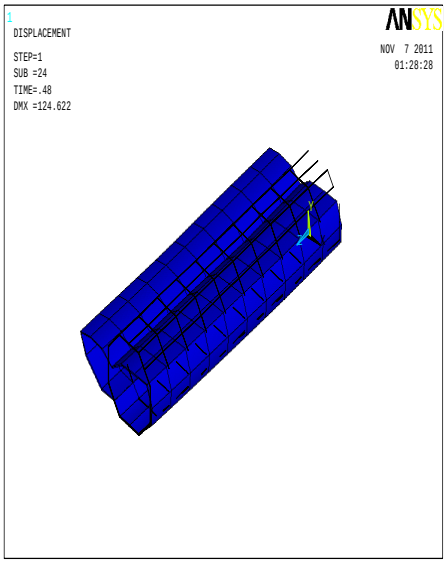

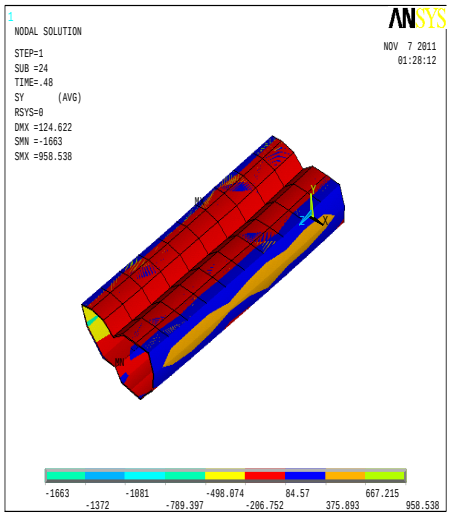

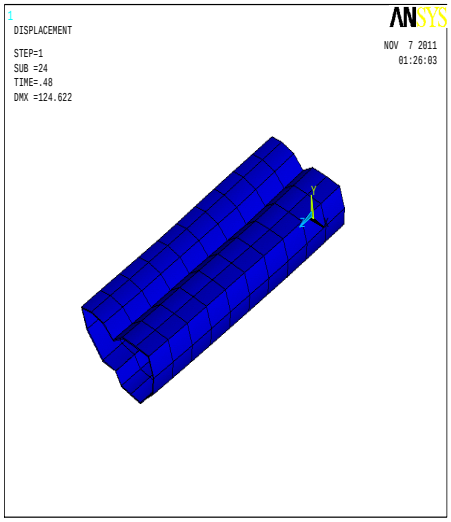

Fig. 15: Distribution of stresses intensity, Maximum displacement in Y direction and bulking of TSB3 beam by ANSYS-9

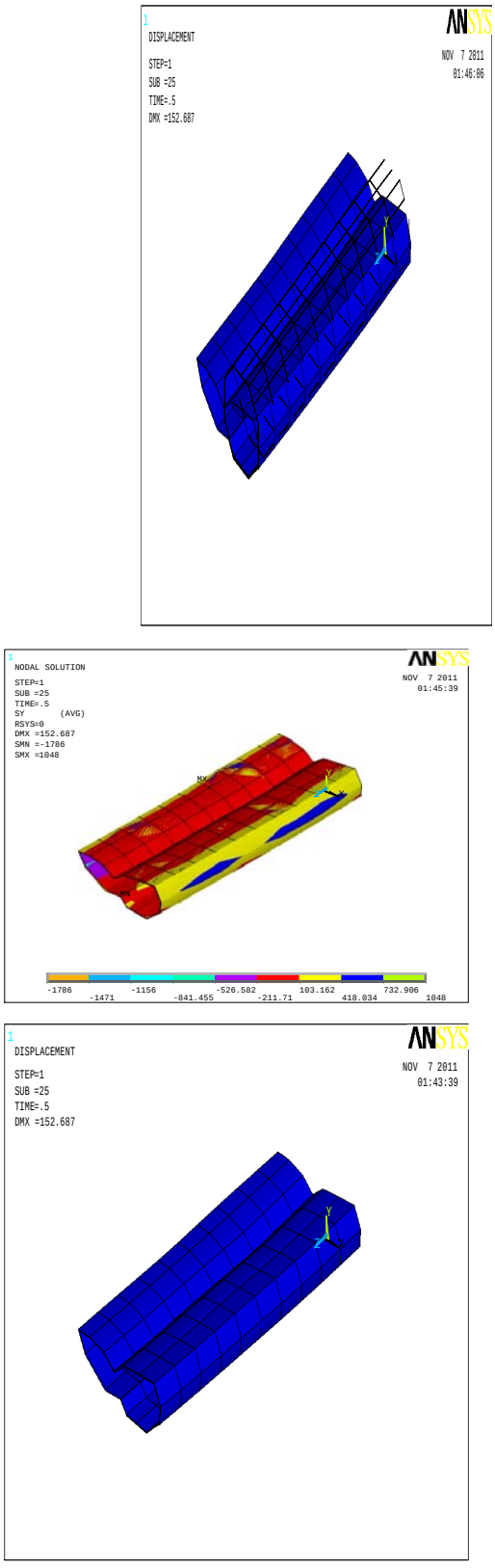

Fig. 16: Distribution of stresses intensitv, Maximum displacement in Y direction and bulking of TSB4 beam bv ANSYS-9.

Conclusion

A strengthening system for steel structures has been developed using intermediate modulus CFRP strips. Substantial stiffness increases from(56.5-100) percent for the five strengthened tubular hollow sections beams that were tested. Strengthening with intermediate modulus CFRP strips in the transverse direction, may also provide ultimate strength increases by delaying the onset of local buckling. By use of ANSYS-9 to create the finite element model, the maximum different between experimental results and ANSYS-9 results is 8.7%.

References

Doi H, et al. Deformation capacity of circular tubular beam-columns reinforced with CFRP subjected to monotonic loading. J Constr Steel 2003;11:431-8[Japan].

Ekiz E. Improving Steel behavior using CFRP warping. Ph.D. Thesis, Department of civil and Environmental Engineering University of Michigan, Ann Arbor, MI,2007.

Hong WS, Zhi MW, Zhi MX, Xing WD. Axial impact behavior and energy absorption efficiency of composite wrapped metal tubes. Int J Impact Eng2000;24:385-401.

Haedir J, Bambach MR, Zhao XL, Grzebieta R. Bending strength of CFRP-strengthened circular hollow steel section. In: Third international conference on FRP composites in civil engineering (CICE) Miami, FL, USA, 2006.

Haedir J, Bambach MR, Zhao XL, Grzebieta R. Behavior of thin-walled CHS beams reinforced by CFRP sheets. Proceeding of the fourth international structural engineering and construction conference (ISEC4), Melbourne, Australia, 2007.

Harries KA., et al. Enhancing stability of structural steel sections using FRP. Thin Walled Struct(2008), doi:10.1016/j.tws.

Jiao H, Zhao XL. CFRP strengthened butt-welded very high strength (VHS) circular steel tubes. Thin-Walled Struct 2004;42(7):963-78.

Teng JG., Hu YM. Behavior of FRP-jacketed circular steel tubes and cylindrical shells under axial compression. Construct Build Mater 2007;21(4):827-38.

Xiao y, He W, Choi K. Confined concrete-filled tubular columns. J Struct Eng, ASCE 2005;131(3):488-97.

Zhao YH, GU W, XU J, Zhang Ht. The strength of concrete-filled CFRP-steel tubes under axial compression. Paper no. 2005-JSC-313, ISOPE Conference, Seoul, June, 2005.

Zhao XL, Fernando ND, AL-Mahaidi R. CFRP strengthened RHS Subjected to transverse end bearing force. Eng Struct 2006;28(11):1555-65.